FLOW PAST OVER CONFINED CYLINDER – A COMPARISON BETWEEN IMMERSED BOUNDARY AND BOUNDARY FITTED COORDINATE

Carlos Alberto de Almeida Vilela, carlosavgeo@yahoo.com
Ricardo Humberto de Oliveira Filho, rhoflho@gmail.com
Rhander Viana, rhanderviana@gmail.com
Andreia Aoyagui Nascimento, andreia.a.nasc@gmail.com
Felipe Pamplona Mariano, fpmariano@emc.ufg.br
Universidade Federal de Goiás, Escola de Engenharias Elétrica, Mecânica e de Computação, Av.: Universitária, 1488, Bloco: A, piso: 3, CEP: 74.605-010, Goiânia-GO.

Abstract. *The purpose of present paper is to show a comparison between Boundary Fitted Coordinate Finite Volume Method (BFC) with steady state formulation and Immersed Boundary Method (IBM) with Fourier pseudospectral transient formulation. Two dimensional confined flow over circular cylinder is solved with incompressible Navier-Stokes equations where BFC method uses a structural non ortogonal grid with QUICK and 2nd Order Upwind schemes for spatial discretization and IBM method uses a regular spacing grid configuration. The problem is performed at various Reynolds number based on channel width and mean inlet velocity, $10 \leq Re \leq 250$ and various blockage ratios $\beta = D/H$, $0.1 \leq \beta \leq 0.9$. Flow streamlines and pressure distribution along the channel, cylinder drag coefficient, inlet-outlet pressure coefficient, stable-instable flow conditions identification are presented as result of analisys.*

***Keywords**: Boundary Fitted Coordinate, Immersed Boundary Method, Finite Volume Method, Pseudospectral Method, Flow over confined cylinder.*

1. INTRODUCTION

A computational fluid dynamic issue is to define how apply boundary conditions with accuracy and computational efficiency in flows over complex geometries. Two classical methods are well known, the finite volumes method (FVM) using boundary fitted coordinates and immersed boundary method (IBM). The boundary conditions in FVM is directly applied, since the mesh is body fitted and adapted exactly over the complex geometry, but is necessary to use a grid generation code to generates the grid over the computational domain. Furthermore, if the geometry moves or changes, the grid generation algorithm should be used in each time step. On the other hand, the IBM arise to solve computational efficiently flow problems over complex and deformable geometries (Peskin, 2002). The grid in IBM is always regular spaced (Fig. 1b), and the geometry is represented by a source term in Navier-Stokes equations. The drawback of this method is the accuracy of results over the geometry, this decreased of accuracy is due the interpolation and distribution functions.

The flow past over cylinders is very common to find in engineering and a particular configuration, of confined cylinder, appears in hydraulic and pneumatic valves and blood stream in veins with greasy walls (Ye et al., 2010). Important information to know about this kind of flow is the velocity and pressure distribution and identification of recirculation zones. In the present work two different numerical methods were used to predict the flow patterns in this situation. Boundary fitted coordinate in finite volume method with QUICK and 2nd Order Upwind discretization schemes and pseudospectral method with immersed boundary approach, which use a cartesian grid.

2. PROBLEM GEOMETRY, BOUNDARY CONDITIONS AND GRID CONFIGURATION

The flow problem geometry consist in a rectangular two dimensional channel with a circular cylinder symmetrically positioned inside it, as described in (Fig. 1).

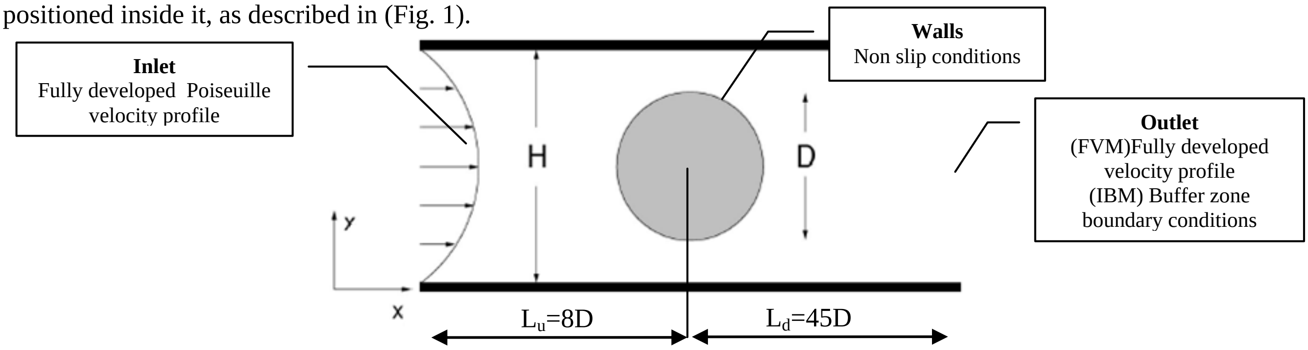

Figure 1. Computational domain and boundary conditions

The inlet profile is considered to be fully developed Poiseuille profile given by:

$$u_y = \frac{\mathrm{Re}}{D}\left(-5,84163\times10^{-3}y^2 + 5,84163\times10^{-4}y\right) \tag{1}$$

where 0≤y≤0,1 ; 0≤D≤0,1

The blockage ratio is defined as the relation between the channel high and the cylinder diameter, $\beta=D/H$, and the Reynolds number is defined as:

$$\mathrm{Re} = \frac{\rho D U_{\max}}{\mu}, \tag{2}$$

where U_{max} is the maximum inlet velocity at channel symmetry.

Figure 2 shows the grid configuration used in finite volume and immersed boundary methods.

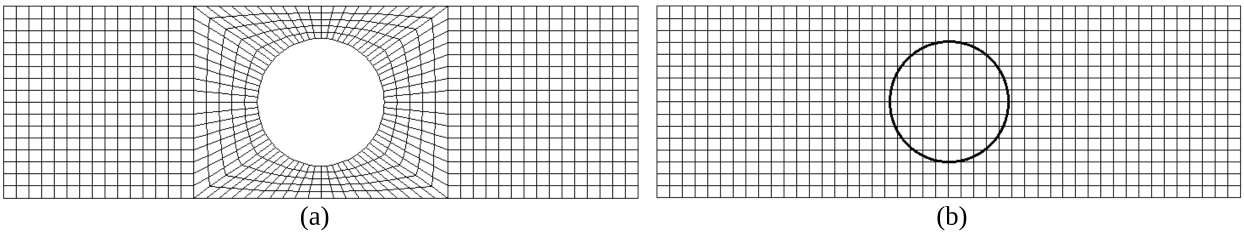

Figure 2. Grid used in (a) Finite Volume Method and (b) Immersed Boundary Method.

For finite volume method to assure the maximum regularity between the grid generated for various blockage ratios, is necessary to create block grids as shows in Fig. (3). Block 1 and 2 are the same for all situations, only the block 3 is adjustable for various blockage ratios.

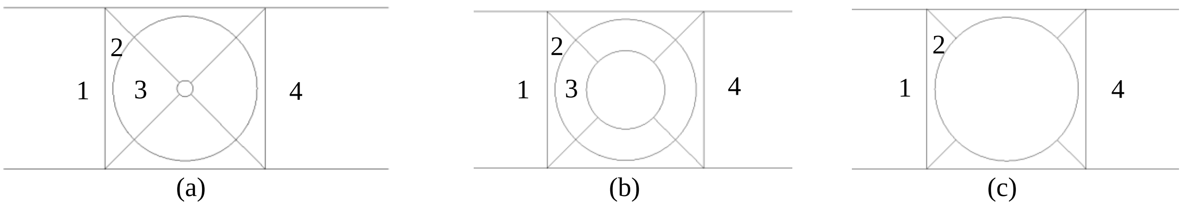

Figure 3. Block diagram grid for finite volume method (a) *β=0,1* (b) *β=0,5* (c) *β=0,9*

Table (1) shows the grid density configuration used in each case.

Table 1: Grid density for finite volume and immersed boundary methods.

	Block 1	Block 2	Block 3	Block 4	Global (BFC)	Global (IBM)
β=0,1	150x50(7500)	50x10(500)	50x40(2000)	1200x50(60000)	79050	900x160(144000)
β=0,3	150x50(7500)	50x10(500)	50x30(1500)	1200x50(60000)	77050	-
β=0,5	150x50(7500)	50x10(500)	50x10(500)	1200x50(60000)	73050	900x160(144000)
β=0,7	150x50(7500)	50x10(500)	50x10(500)	1200x50(60000)	73050	-
β=0,9	150x50(7500)	50x10(500)	-	1200x50(60000)	71050	900x160(144000)

2. MATHEMATICAL MODELING

In the present section two-dimensional Navier-Stokes and continuity equations are presented. Furthermore, the formulation of Immersed Boundary Method (IBM) based in multi-direct forcing (Wang et al., 2007) coupled with Fourier pseudospectral method (Mariano, 2010b).

2.1 Mathematic model for the fluid

The flow is governed by conservation momentum equation (Eq. 3) and the continuity equation (Eq. 4). The equations that model the problem are presented in theirs tensorial form:

$$\frac{\partial u_l}{\partial t}+\frac{\partial (u_l u_j)}{\partial x_j}=-\frac{\partial p}{\partial x_l}+\nu\frac{\partial^2 u_l}{\partial x_j \partial x_j}+f_l \tag{3}$$

$$\frac{\partial u_j}{\partial x_j}=0 \tag{4}$$

where $\frac{\partial p}{\partial x_l}=\frac{1}{\rho}\frac{\partial p^*}{\partial x_l}$; p^* is the static pressure in [N/m^2]; u_l is the velocity in l direction in [m/s]; $f_l=\frac{f_l^*}{\rho}$; f_l^* is the term source in [N/m^3]; ρ is the density; ν is the cinematic viscosity in [m^2/s]; x_l is the spatial component (x,y) in [m] and t is the time in [s]. The initial condition is any velocity field that satisfies the continuity equation.

2.2 Mathematic model for Immersed Boundary Method

In IBM method the information of the fluid/solid interface (domain Γ) is passed to the eulerian domain (Ω) for addition of the term source to Navier-Stokes equations. This term plays a role of a body force that represents the boundary conditions of the immersed geometry (Goldstein *et al*, 1993). The source term is defined in all domain Ω, but presents different values from zeros only in the points that coincide with the immersed geometry (Eq. 5), enabling that the eulerian field perceives the presence of solid interface (Enriquez-Remigio and Silveira Neto, 2007).

$$f_l\left(\vec{x},t\right)=\begin{cases}F_l\left(\vec{x}_k,t\right) & \text{if } \vec{x}=\vec{x}_k\\ 0 & \text{if } \vec{x}\neq\vec{x}_k\end{cases} \tag{5}$$

where $\vec{x}$ is the position of the particle in the fluid and $\vec{x}_k$ is the position of a point in solid interface (Fig. 4).

The lagrangian force field is calculated by direct forcing methodology, which was proposed by Uhlmann (2005). One of the characteristics of this model is modeling the non-slip boundary condition on immersed interface.

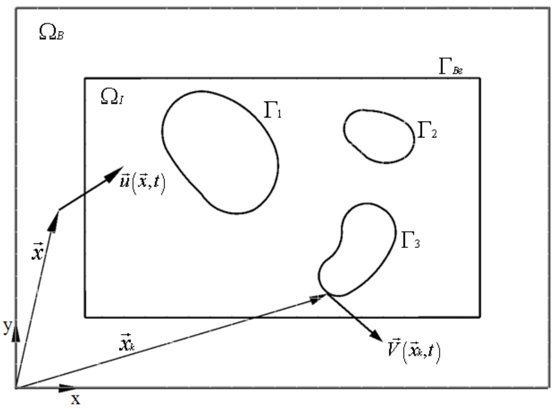

Figure 4. Schematically representation of eulerian and lagrangian domain (Mariano *et al*, 2010b).

The Eq. (5) can be conclude that the field $f_l\left(\vec{x},t\right)$ is discontinuous, which can be numerically solved only when there are coincidence between the points that compose the interface domain and the compose the fluid domain. In cases there is no coincidence between these points, (complex geometries), it is necessary to distribute the function $f_l\left(\vec{x},t\right)$ on its neighborhoods. Just by calculating the Lagrangian force field $F_l\left(\vec{x}_k,t\right)$, it can be distributed and thus, transmitted the information geometry presence for Eulerian domain, these functions can be found in Griffith and Peskin, (2005).

The Lagrangean force field, in the present study, is calculated by the direct forcing method (DFM), which was proposed by Wang et al. (2008). One of the characteristics of this model is that is not necessary to use *ad-hoc* constants and allows the non-slip condition modeling on immersed interface. The Lagrangean force, $F_l(\vec{x}_k,t)$, is available by momentum conservation equation over a fluid particle that is joined in the fluid-solid interface:

$$F_l(\vec{x}_k,t)=\frac{\partial u_l}{\partial t}(\vec{x}_k,t)+\frac{\partial}{\partial x_j}(u_l u_j)(\vec{x}_k,t)+\frac{\partial p}{\partial x_l}(\vec{x}_k,t)-\nu\frac{\partial^2 u_l}{\partial x_j \partial x_j}(\vec{x}_k,t). \tag{6}$$

The values of $u_l(\vec{x}_k,t)$ and $p(\vec{x}_k,t)$ are given by interpolation of velocities and pressure, respectively, of the Eulerian points near the immersed interface (Lima e Silva et al., 2003). For Lagrangean points, $\vec{x}_k$, at the immersed boundary, we have:

$$F_l(\vec{x}_k,t)=\frac{u_l(\vec{x}_k,t+\Delta t)-u_l^*(\vec{x}_k,t+\Delta t)+u_l^*(\vec{x}_k,t+\Delta t)-u_l(\vec{x}_k,t)}{\Delta t}+RHS(\vec{x}_k,t), \tag{7}$$

where $u*$ is a temporary parameter, as defined in Wang *et al.* (2008), Δt is the time step and *RHS* are the terms of the right hand side of Eq. (6). The Eq. (7) is solved by Eqs. (8) and (9) at the same time step:

$$\frac{u_l^*(\vec{x}_k,t+\Delta t)-u_l(\vec{x}_k,t)}{\Delta t}+RHS(\vec{x}_k,t)=0\,, \tag{8}$$

$$F_l(\vec{x}_k,t)=\frac{u_l(\vec{x}_k,t+\Delta t)-u_l^*(\vec{x}_k,t+\Delta t)}{\Delta t}\,, \tag{9}$$

where $u_l(\vec{x}_k,t+\Delta t)$ is the immersed boundary velocity, *i.e.* the specific boundary condition, normally known.

Equation (8) is solved in the Eulerian domain in the Fourier spectral space, *i.e.* the solution of Eq. (4) with $f_l=0$. $u_l^*(\vec{x}_k,t+\Delta t)$ is interpolated for the Lagrangean domain and became $u_l(\vec{x}_k,t+\Delta t)$ and it is computed on Eq.12. Then $F_l(\vec{x}_k,t)$ is smeared for Eulerian mesh. Finally, the Eulerian velocity is updated by Eq. 8:

$$u_l(\vec{x},t+\Delta t)=u_l^*(\vec{x},t+\Delta t)+\Delta t\cdot f_l(\vec{x},t) \tag{10}$$

2.3 Fourier Pseudospectral Method

The methodology used by solving Navier-Stokes equations with IBM is the Fourier pseudospectral method (Canuto et al., 2007). It consists in applied the Fourier transformed in Eqs. (1) and (2), given:

$$ik_j\hat{u}_j=0 \tag{11}$$

$$\frac{\partial\hat{u}_l(\vec{k},t)}{\partial t}+\nu k^2\hat{u}_l(\vec{k},t)=\hat{f}_l(\vec{k},t)-ik_j\wp_{lm}\int_{\vec{k}=\vec{r}+\vec{s}}\hat{u}_l(\vec{r},t)\hat{u}_l(\vec{k}-\vec{r},t)d\vec{r} \tag{12}$$

The Navier-Stokes equations, Eq. 12, are transformed to spectral space using the Discrete Fourier Transform (DFT), which is defined by Briggs and Henson (1995) and computationally performed by Fast Fourier Transform (FFT) given in Takahashi (2006). The boundary conditions are imposed by coupling IBM, this methodology is named IMERSPEC (Mariano et al. 2010).

The convolution integral to solve the non-linear term was solved using the skew-symmetric approach (Canuto et al., 2006). And the temporal evolution is performed by low dispersive and low dissipative explicit forth order optimized Runge-Kutta (Allampalli et al. 2009).

3. RESULTS

Figure 5 presents the solution of the instantaneous horizontal velocity field superimposed by vector velocity near the cylinder using the IBM for two different β ratios at *Re=100*. It is possible to verify the effect of β over the recirculation zone, that decrease when β increase. In Fig. 5 can be noted the virtual flow generated by immersed boundary method within the cylinder, which appears to close momentum equation (Eq. 3).

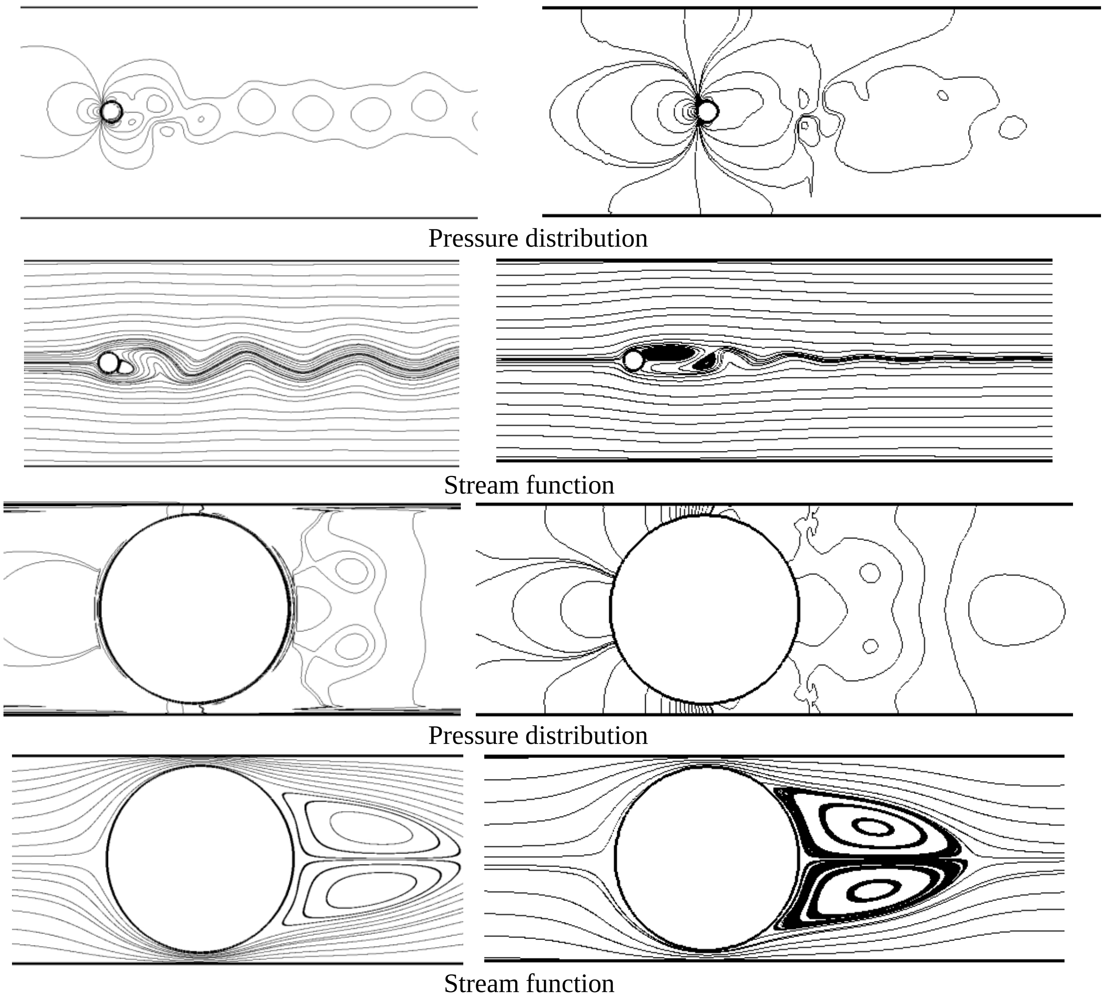

Figure 5. Solution obtained using IBM(left) BFC(right) for flow over cylinder to *Re=100* and (a) $\beta=0{,}1$, and (b) $\beta=0{,}9$.

Figure 5 shows the streamlines obtained by finite volume simulation using BFC, for the same parameters using in IBM. The solutions obtained in case of FVM is steady and the recirculation bubble appears downstream the cylinder. For $\beta=0{,}9$ the recirculation is less than $\beta=0{,}1$ as expected at *Re=100.*

In order to compare the solutions of IBM and BCF, two parameters are presented in Tab. 1, the drag and pressure coefficients given by Eqs. 13 and 14, respectively, for different Reynolds numbers (Eq. 2) and different aspect ratios (β).

$$C_d = \frac{F_x}{0{,}5\rho U_{\max}^2 D}, \tag{13}$$

$$C_p = \frac{\left(P_{in} - P_{out}\right)}{0{,}5\rho U_{\max}^2}, \tag{14}$$

where F_x is the force in horizontal direction over the cylinder surface, in IBM is provide by Eq. 9 and in BFC is performed by a surface integral, P_{in} and P_{out} are the mean pressure at inlet and outlet of domain.

In Fig. 6 is presented the comparison of pressure and drag coefficients, for different aspect ratios, β. The results are closed for β=0.5 and β=0.9, however for β=0.1 we verify differences. This behavior can be explained by the insufficiency of points in the interior of cylinder modeled by immersed boundary, *i.e.*, to well represent the internal flow of immersed geometry the IBM requires a high density of points.

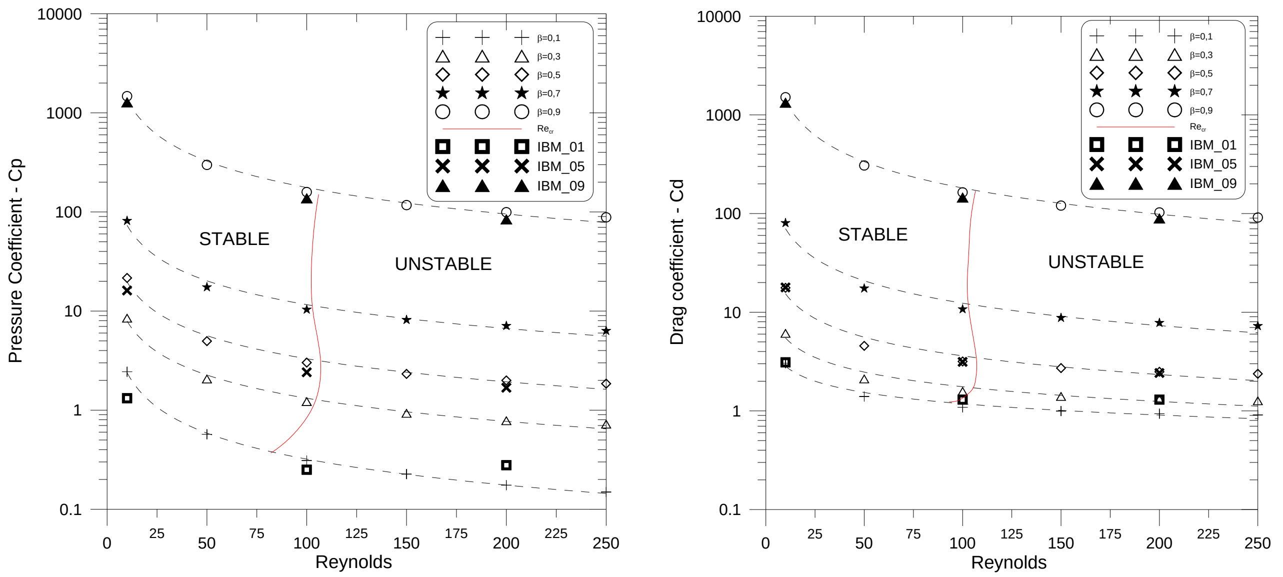

Figure 6. Comparison of pressure (a) and drag (b) coefficients between IBM and BFC for different aspect ratios.

In all simulations performed using IBM, in the present paper, the number of points are constant and to change a Reynolds number we adapted the cylinder diameter. This way, for large aspect ratios the cylinder has more points in its interior.

Other factor that explained the differences in pressure coefficient are the periodic boundary conditions of Fourier pseudospectral method. For modeling the boundary conditions, inlet and outlet, of domain we imposed the buffer zone this procedure modified the pressure field, and can be solved using a large domain. For more details report to Mariano, (2010a).

Figure 6 also is presented a study of the stability region for different blockage ratios. In the left of red line define the region where the flow is stable, without oscillations. And in other side is the range of Reynolds number that the flow is unstable or present the periodical ocillations.

4. CONCLUSIONS

In the present paper a comparison between immersed boundary method and boundary fitted coordinate are performed in flows over confined cylinders. For these simulations the results show that BFC is more efficient because the IBM require more mesh points to well represent the cylinder interface.

It is important highlight that the interface is static, when we have interfaces that move or deform the mesh generation of BFC is not attractive.

5. ACKNOWLEDGEMENTS

The authors thank the School of Engineering Electrical, Mechanical and of Computational (EMC) of the University Federal of Goiás (UFG) and FAPEG for financial support.

6. REFERENCES

Allampalli, V., Hixon, R., Nallasamy, M., Sawyer, S., 2009, "High-accuracy large-step explicit Runge-Kutta (HALE-RK) schemes for computational aeroacoustics. Journal of Computational Physics, Vol. 228, pp. 3837-3850.

Canuto, C., Hussaini, M.Y., Quarteroni, A. and Zang, T.A., 2007, "Spectral methods: evolution to complex geometries and applications to fluid dynamics", Ed: Springer-Verlag, New York, United States, 596p.

Enriquez-Remigio, S. and Silveira-Neto, A., 2007, "A new modeling of fluid-structure interaction problems through immersed boundary method/virtual physical model (IBM/VPM)", Proceedings of the 19th Brazilian Congress of Mechanical Engineering, Vol.1, pp. 1-10.

Ferziger, J.H. and Peric, M., 2002. “Computational Methods for Fluid Dynamics”. Ed: Springer Verlag, 3rd edition, Berlin, Germany.

Fornberg, B., 1980. “A numerical study of steady viscous flow past a circular cylinder”. Journal of Fluid Mechanics, Vol. 98, No. 4, pp. 819–855.

Goldstein, D., Handler, R. and Sirovich, L., 1993. “Modeling a no-slip flow with an external force field”. Journal Computational Physics, Vol. 105, pp. 354-366.

Griffith, B.E. and Peskin, C.S., 2005, “On the order of accuracy of the immersed boundary method: higher order convergence rates for sufficiently smooth problems”, Journal Computational Physics, Vol.208, pp. 75-105.

Mariano, F.P., Moreira, L.Q. and Silveira Neto, A., 2010a, “Mathematical Modeling of non-periodic flows using Fourier pseudo-spectral and immersed boundary methods”, Proceedings of the 5th European Conference on Computational Fluid Dynamics, Vol.1, Lisbon, Portugal, pp. 1-17.

Mariano, F.P., Moreira, L.Q., Silveira-Neto, A., Silva, C.B. da, Pereira, J.C.F., 2010b, “A new incompressible Navier-Stokes solver combining Fourier pseudo-spectral and immersed boundary method. Computer Modeling in Engineering Science, v. 59, p. 181-216.

Park, J., Kwon, K. and Choi, H., 1998. “Numerical solutions of flow past a circular cylinder at Reynolds numbers up to 160”. KSME International Journal, Vol. 12, No. 6, pp. 1200–1205.

Patankar, S.V., 1980. “Numerical Heat Transfer and Fluid Flow”. Ed: McGraw-Hill, New York.

Peskin, C.S., 2002, “The immersed boundary method”, Acta Numerica, Vol.11, pp. 479–517.

Sahin, M., and Owens, R.G., 2004. “A numerical investigation of wall effects up to high blockage ratios on two-dimensional flow past a confined circular cylinder”. Physics of Fluid, Vol. 16, No. 5.

Wang Z., Fan J. and Luo, K., 2008, “Combined multi-direct forcing and immersed boundary method for simulating flows with moving particles”, International Journal of Multiphase Flow, Vol.34, pp. 283-302.

Ye, T., Mittal, R., Udaykumar, H.S. and Shyy, W., 1999. “An accurate cartesian grid method for viscous incompressible flows with complex immersed boundaries”. Journal of Computational Physics, Vol. 156, pp. 209–246.

7. RESPONSIBILITY NOTICE

The authors are the only responsible for the printed material included in this paper.